PROCEEDINGS OF SCIENCE

CMS Silicon Strip Tracker Performance in Run 3

Jindřich Lidrych[a,*] **for the CMS Collaboration**

[a] *Centre for Cosmology, Particle Physics and Phenomenology, Université catholique de Louvain, Louvain-la-Neuve, Belgium*

E-mail: jindrich.lidrych@cern.ch

The CMS tracking system is the world's largest silicon tracker, comprising 1,856 pixel and 15,148 strip modules. In these proceedings, we present the performance of the silicon strip tracker during data taking in LHC Run 3, based on proton-proton collisions at the center-of-mass energy of 13.6 TeV. Key performance metrics such as signal-to-noise ratio, hit efficiency, resolution, and evolution of bad module components will be shown. The results demonstrate that the tracker maintained excellent performance throughout Run 3 so far, ensuring high-quality tracking crucial for CMS physics analyses.

The European Physical Society Conference on High Energy Physics (EPS-HEP2025)
7-11 July 2025
Marseille, France

*Speaker

 ISSN 1824-8039 . Published by SISSA Medialab.

PoS(EPS-HEP2025)500

1. Introduction

The CMS tracking system is the world's largest silicon tracker, comprising 1,856 pixel and 15,148 strip modules. The CMS Silicon Strip Tracker (SST) [1] was installed in the CMS experiment [2] in 2007. Together with the pixel detector, the SST records charge deposits (hits) at discrete points along the paths of charged particles produced in proton-proton collisions. These hits are then used to reconstruct the trajectories of charged particles traversing the detector up to a pseudorapidity of $|\eta| < 2.5$.

The SST occupies a cylindrical volume of 6 m in length and 2.2 m in diameter around the beam line, with an active area of 200 m^2. The detector geometry is shown in Figure 1. The central part of the SST has a barrel-type geometry, consisting of ten layers of silicon modules with their surfaces parallel to the beam axis. This barrel region is composed of the Tracker Inner Barrel (TIB) and the Tracker Outer Barrel (TOB), comprising four and six layers of silicon modules, respectively. The forward regions on each side are complemented by three smaller disks forming the Tracker Inner Disks (TID) and nine disks forming the Tracker Endcaps (TEC). Each TID consists of three rings, while the disks in each TEC contain between four and seven rings.

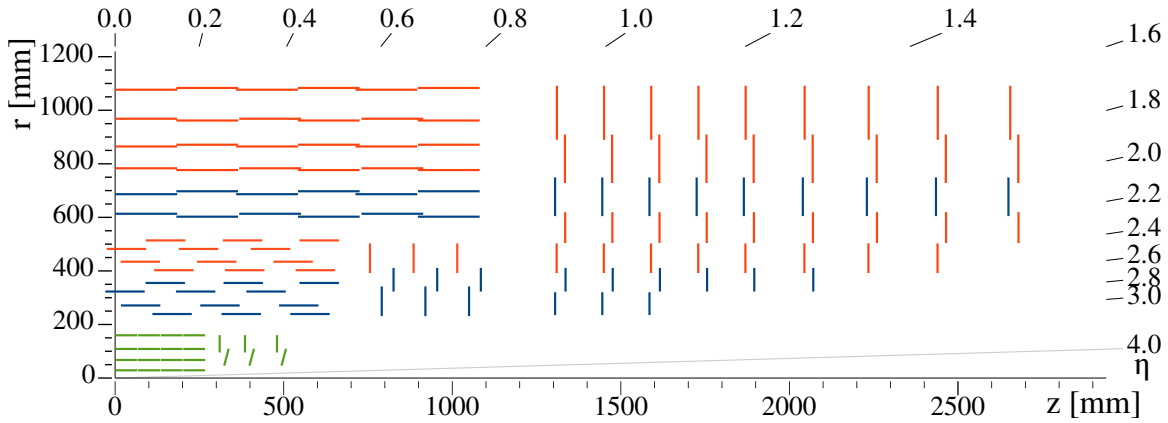

Figure 1: An $r - z$ view of one quarter of the CMS silicon strip tracker. Layers with stereo modules are drawn as blue lines, while layers with single modules as red lines. The Phase-1 pixel detector is shown in green. Taken from Ref. [3].

Silicon modules with a single sensor thickness of 320 μm are used in the TIB, TID, and the first four inner rings of the TEC, while 500 μm sensors are used in the modules of the last five outer rings of the TEC. The first two layers of the TIB and TOB, and the two and three rings of the TID and TEC, respectively, are made of double-sided modules. These double-sided, or stereo, modules consist of two detector modules glued together in a back-to-back configuration, with the strips of one module rotated by 100 mrad relative to the other. This arrangement enables the measurement of three-dimensional hit positions, specifically, the radial coordinate (r) in the disks and the longitudinal coordinate (z) in the barrel.

The silicon sensors are of the p-on-n microstrip type [4]. The spacing between the individual p implants of the readout strips (the pitch) varies between 80 and 205 μm, depending on the radial position in the tracker, and generally increases with radius [3].

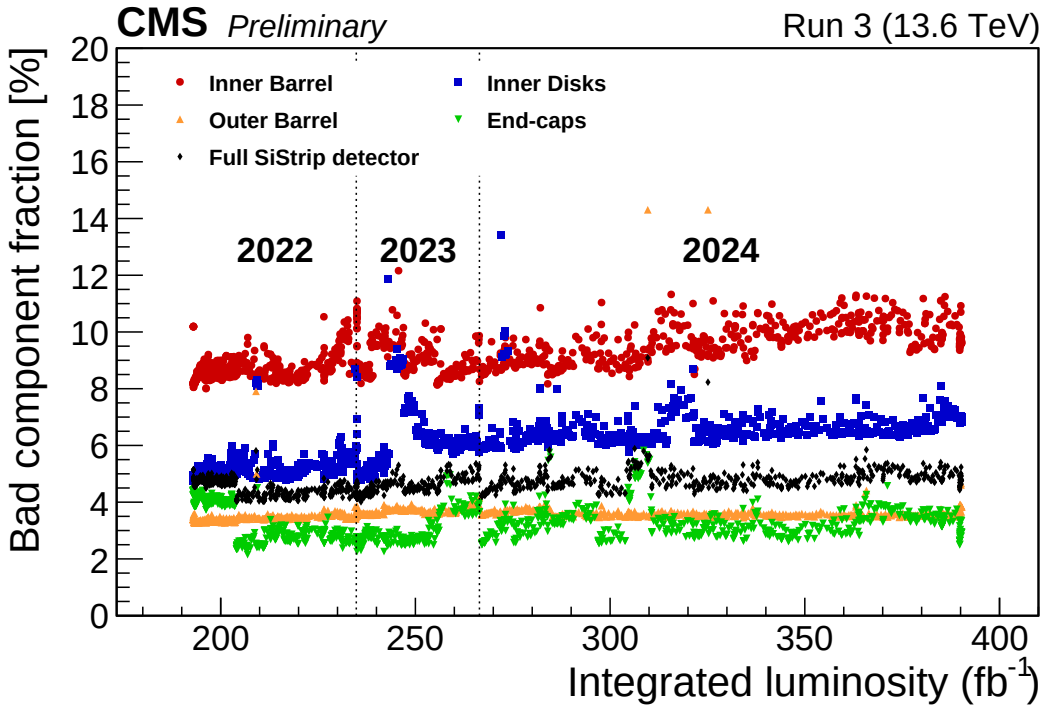

Figure 2: The evolution of the global fraction of module components flagged as bad for offline reconstruction for pp collisions at a centre of mass energy of 13.6 TeV as a function of integrated delivered luminosity. The data include 2022, 2023, and 2024 data-taking periods. The initial offset of 193 fb^{-1} corresponds to the integrated luminosity of Run 1 and Run 2. Taken from Ref. [5].

2. Detector status in Run 3

The status of the SST is continuously monitored. When noisy or inefficient electronic channels are identified, this information is propagated to the offline data processing so that these channels can be masked before track reconstruction. Figure 2 shows the evolution of the global fraction of module components flagged as bad for offline reconstruction as a function of the integrated delivered luminosity. The data include the 2022, 2023, and 2024 data-taking periods. The initial offset of 193 fb^{-1} corresponds to the integrated luminosity accumulated during Run 1 and Run 2. The drop in the bad module fraction around 205 fb^{-1} is due to the recovery of a cooling loop in the TEC. The jump for Inner Disks around 245 fb^{-1} is due to a number of modules whose power supplies were turned off. The several jumps observed in the bad-module fraction correspond to periods when groups of modules were temporarily powered off. Overall, the average fraction of bad components is slightly above 4%.

3. Performance in Run 3

The performance of the SST is also continuously monitored. Performance metrics such as the signal-to-noise ratio, hit efficiency, and resolution are commonly used as figures of merit to assess the detector performance during data-taking periods.

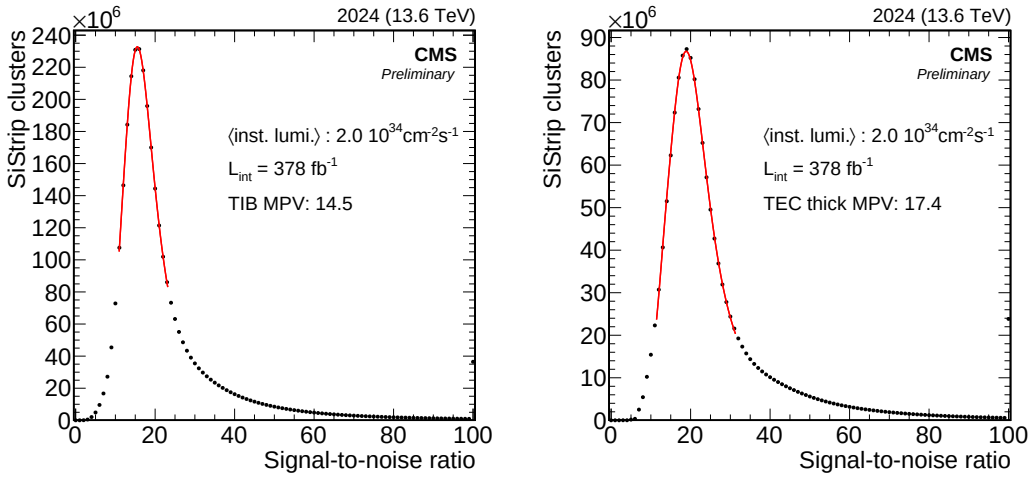

Figure 3: The overall signal-to-noise ratio for TIB (left) and TEC 500 μm sensors (right), corrected for path length inside the silicon, is shown for the end of the 2024 run with 13.6 TeV pp collisions where the silicon strip tracker was operated in deconvolution mode [6], and cooled at -25°C. The position of the MPV of the peak is given, estimated from a fit with a Landau convoluted with a Gaussian distribution. The lifetime integrated luminosity of high-energy pp collisions delivered by the LHC was 378 fb^{-1}. Taken from Ref. [5].

3.1 Signal-to-noise ratio

The signal-to-noise ratio (S/N) is computed for clusters associated with reconstructed tracks. The signal is defined as the total charge of the cluster in ADC counts (sum of all contributing strips after pedestal subtraction), and the noise corresponds to the quadratic sum of the individual strip noise values provided by the calibration [3]. Two example distributions of the S/N are shown in Figure 3 for the TIB and the thick sensors of the TEC. The S/N is corrected for the path length within the silicon. The position of the most probable value (MPV) is obtained from a fit with a Landau function convoluted with a Gaussian distribution. Figure 4 shows a summary of the overall signal-to-noise ratio for the individual parts of the SST since Run 2, measured as a function of the integrated delivered luminosity. The measurements for the TEC sensors are split by sensor thickness. A linear fit to the data shows that the S/N decreases linearly with increasing integrated luminosity, as expected. The observed decrease reflects the impact of radiation damage, which reduces charge collection efficiency and increases strip noise. In addition, the S/N values extrapolated from the fits to the end of Run 3 remain well above the design specifications and are sufficiently good enough to ensure high-quality physics data taking.

3.2 Hit resolution

The strip hit resolution is computed using hits in overlapping modules of the same layer, employing the so-called pair method. Only tracks with a transverse momentum of $p_{\mathrm{T}} > 3$ GeV are used. In addition, the tracks are required to have at least eight valid hits and a track-fit χ^2 probability greater than or equal to 10^{-3}. The selected hit pairs are required to have a cluster width of at most four strips and to correspond to clusters of the same width in both modules. The propagation distance from one detector surface to the next must be smaller than 7 cm, i.e. only pairs within the same

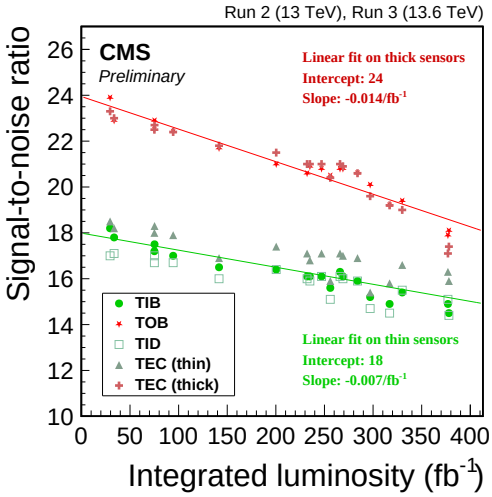

Figure 4: The overall signal-to-noise ratio for the individual parts of the SST measured in pp collisions since Run 2 is reported as a function of the integrated delivered luminosity. Measurements for the Tracker Endcaps have been split by sensor thickness (320 μm or 500 μm). The S/N scales with integrated luminosity. The data were fitted with a linear function. Taken from Ref. [5].

layer are considered. Finally, the uncertainty on the predicted distance in the bending coordinate between the two hits must be smaller than 25 μm. In order to separate the impact of hit resolution from the intrinsic resolution of track fit itself, the difference in distance between the measured and predicted hits in the two sensors is used, $\Delta_{\text{meas-pred}} = (\text{meas}_1 - \text{pred}_1) - (\text{meas}_2 - \text{pred}_2) = \Delta x_{\text{meas}} - \Delta x_{\text{pred}}$. Assuming the difference in prediction is an independent quantity, and the hit resolution in both sensors is the same, the Root Mean-Square of this distribution will be given by $\sigma^2_{\text{meas}-\text{pred}} = 2\sigma^2_{\text{hit}} + \sigma^2_{\text{pred}}$, where σ^2_{pred} is given by the RMS of the difference of predicted position in both sensors (Δx_{pred}). Isolating for hit resolution, we then have the hit resolution in a single sensor as

$$\sigma_{\text{hit}} = \sqrt{\frac{\sigma^2_{\text{meas}-\text{pred}} - \sigma^2_{\text{pred}}}{2}}. \tag{1}$$

Figure 5 shows a schematic illustration of the overlap method used to measure the intrinsic hit resolution.

Figure 6 shows the strip hit resolution for proton–proton collision runs in 2024, during which the SST was operated in deconvolution mode [6], i.e. under nominal conditions. The theoretically expected resolution from a binary readout tracking detector, i.e. a hit/no-hit system, is also shown for comparison. By measuring the fraction of charge collected by adjacent strips, the hit position can be interpolated more precisely, resulting in a resolution significantly better than the binary limit.

3.3 Hit efficiency

The hit efficiency is defined as the ratio of detected hits to the number of expected hits associated with a track. Regular measurements of the hit efficiency are performed using both collision and cosmic-ray data. This measurement makes use of only high-quality tracks. Tracks are required to have a transverse momentum of $p_{\text{T}} > 1$ GeV and at least eleven valid hits. The probability

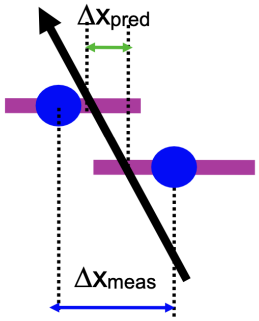

Figure 5: Schematic illustration of the overlap method used to measure the hit resolution. The difference between measured and track-predicted positions in two overlapping sensors ($\Delta_{meas-pred}$) is used to extract the intrinsic hit resolution.

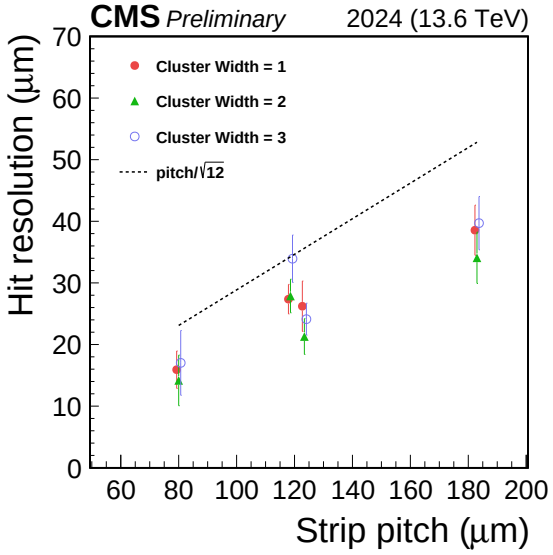

Figure 6: Strip hit resolution is shown for 13.6 TeV pp collisions run in 2024 where the silicon strip tracker was operated in deconvolution mode (nominal conditions). Strip hit resolution is derived by selecting pairs of hits in different types of overlapping sensors, and are computed separately for clusters of width 1, 2, and 3 strips. Taken from Ref. [5].

of false track-to-cluster associations is reduced by considering only tracks that have no additional trajectories within 5 mm.

Figure 7 shows the hit efficiency measured as a function of the instantaneous luminosity for a standard fill from proton-proton collisions taken in May 2024, where the luminosity was below 2.2×10^{34} cm^{-2}s^{-1}. Separate measurements have been performed for the TIB and TOB layers. The efficiency is computed only for operational detector elements, excluding known bad or inactive modules and strips. As shown in Figure 7, the hit efficiency is well above 98.5% and 98% for the innermost layers of the TIB and TOB, respectively. The hit efficiency decreases approximately linearly with increasing instantaneous luminosity, with Layer 1 of the TOB showing the strongest

reduction. The inefficiency arises mainly from heavily ionizing particles that saturate the APV25 readout, causing short periods of insensitivity over a few bunch crossings. This effect is most pronounced in the innermost TOB layer.

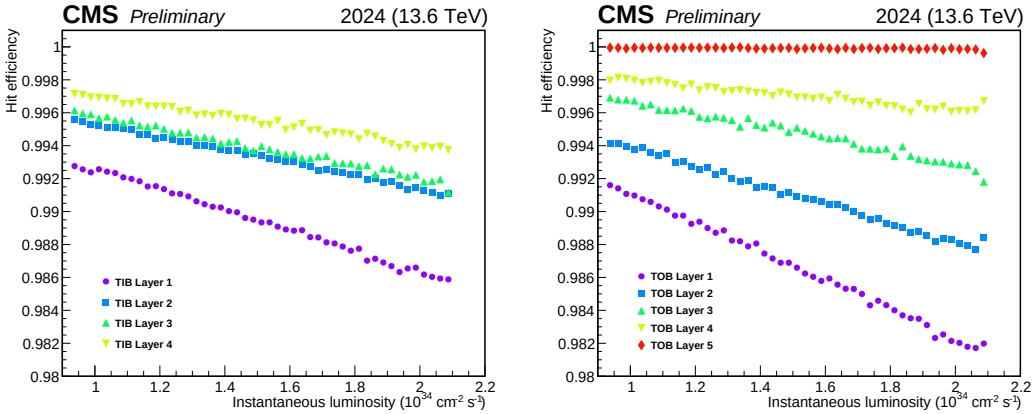

Figure 7: Hit efficency of SST from four tracker inner barrel (TIB) layers (left) and five tracker outer barrel (TOB) layers (right) as a function of the instantaneous luminosity. Data are from a 13.6 TeV proton-proton fill recorded in May 2024, where the luminosity was below 2.2×10^{34} cm^{-2}s^{-1} . Taken from Ref. [7].

4. Summary

In these proceedings, the performance of the Silicon Strip Tracker during data taking in LHC Run 3, based on proton–proton collisions at a center-of-mass energy of 13.6 TeV, has been presented. Key performance metrics such as the signal-to-noise ratio, hit efficiency, spatial resolution, and the evolution of bad module components have been shown. After more than twelve years of operation and an integrated luminosity approaching 400 fb^{-1}, the results demonstrate that the tracker has maintained excellent performance, ensuring the high-quality tracking essential for CMS physics analyses.

References

[1] CMS Collaboration, *The CMS Tracker*, Technical Design Report, CERN-LHCC-98-006, CERN, Geneva (2000).

[2] CMS Collaboration, *The CMS Experiment at the CERN LHC*, *JINST* **3** (2008) S08004.

[3] CMS Collaboration, *Operation and performance of the CMS silicon strip tracker with proton-proton collisions at the CERN LHC*, *JINST* **20** (2025) P08027 [2506.17195].

[4] M. Raymond, M. French, J. Fulcher, G. Hall, L. Jones, K. Kloukinas et al., *The APV25 0.25 µm CMOS readout chip for the CMS Tracker*, in *2000 IEEE Nuclear Science Symposium*, vol. 2, pp. 9/113–9/118, (2000).

[5] CMS Collaboration, *CMS Silicon Strip Tracker Performance Results with 2024 Data*, Detector Performance Note, CMS-DP-2025-020, CERN (May, 2025).

[6] S. Gadomski, G. Hall, T. Hogh, P. Jalocha, E. Nygard and P. Weilhammer, *The Deconvolution method of fast pulse shaping at hadron colliders*, *Nucl. Instrum. Meth. A* **320** (1992) 217.

[7] CMS Collaboration, *CMS Silicon Strip Tracker Performance Results with Early 2024 Data*, Detector Performance Note, CMS-DP-2024-101, CERN (October, 2024).